



Was there a glacial outburst flood in the Torngat Mountains during Marine Isotope Stage 3?

Tamara Pico^{1*}, Jane Willenbring², April S. Dalton³, Sidney Hemming⁴

¹ Earth & Planetary Sciences, 1156 High St, University of California, Santa Cruz, Santa Cruz, CA, 95064, USA

² Earth, Energy, & Environmental Sciences, 50 Jane Stanford Way, Building 320, Room 325, Stanford University, Stanford, CA, 94305-2215, USA

³ Department of Physical Geography, Opletalova 38, 110 00 Staré Město, Charles University, Prague, Czech Republic

⁴ 413 Comer, Columbia/Lamont-Doherty Earth Observatory, 61 Rte 9W, Palisades, NY, 10964, USA

*Corresponding email: tpico@ucsc.edu

ABSTRACT

We report previously unpublished evidence for a Marine Isotope Stage 3 (MIS 3; 60-26 ka) glacial outburst flood in the Torngat Mountains (northern Quebec/Labrador, Canada). We present ¹⁰Be cosmogenic exposure ages from legacy fieldwork for a glacial lake shoreline with evidence for outburst flooding in the Torngat Mountains, with a minimum age of 36 ± 3 ka (we consider the most likely age, corrected for burial, to be $\sim 56 \pm 3$ ka). This shoreline position and age can potentially constrain the Laurentide Ice Sheet margin in the Torngat Mountains. This region, considered a site of glacial inception, has no published dated geologic constraints for high-elevation MIS 3 ice margins. We estimate the freshwater flux associated with the inferred glacial outburst flood using high-resolution digital elevation maps corrected for glacial isostatic adjustment. Using assumptions about the ice-dammed locations we find that a freshwater flood volume of $1.14 \times 10^{12} \text{ m}^3$ could have entered the Hudson Strait. This glacial outburst flood volume could have contributed to surface ocean freshening to cause a measurable meltwater signal in $\delta^{18}\text{O}$ records, but would not necessarily have been associated with substantial ice rafted debris.



30 Future work is required to refine estimates of the size and timing of such a glacial outburst flood.
31 Nevertheless, we outline testable hypotheses about the Laurentide Ice Sheet and glacial outburst
32 floods, including possible implications for Heinrich events and glacial inception in North
33 America, that can be assessed with additional fieldwork and cosmogenic measurements.

34

35 **SHORT SUMMARY:**

36 We present data from fieldwork completed in 2002 for a glacial lake in the Torngat Mountains
37 (Northern Quebec and Labrador, Canada). We dated the lake to $\sim 56 \pm 3$ ka and estimated the
38 freshwater volume that may have been released during an outburst flood. The location of this
39 glacial lake is surprising because the Torngat Mountains are considered a site of glacial
40 inception, and this shoreline suggests the region was not ice-covered throughout the North
41 American ice sheet growth phase.

42

43 **MOTIVATION**

44

45 MIS 3 Heinrich events, ice sheets, and climate variability

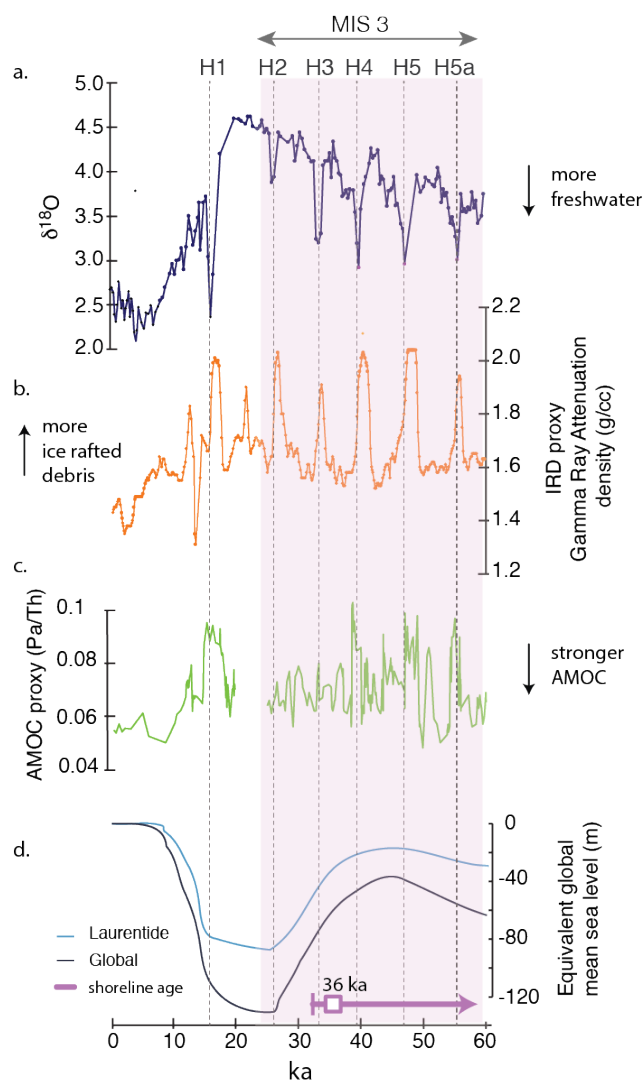
46 Millennial-scale climate oscillations in the Northern Hemisphere are prominent features of
47 Marine Isotope Stage 3 (MIS 3; 60-26 ka). Abrupt iceberg discharge episodes, known as
48 Heinrich events (Hemming, 2004), passed through the Hudson Strait repeatedly during MIS 3.
49 The cause for Heinrich events remains enigmatic, especially in relation to synchronous
50 temperature changes recorded in Greenland ice cores (Dansgaard-Oeschger events; Bond *et al.*,
51 1993). These massive ice-rafted debris (IRD) episodes are associated with freshwater anomalies
52 in the North Atlantic, alluding to the potential role of Heinrich events in modulating Atlantic



53 overturning circulation, and thereby global climate change (Henry et al., 2016; Seidenkrantz et
54 al., 2021) (Figure 1).

55

56 A variety of mechanisms have been proposed to explain Heinrich events, including cycles of
57 large ice sheets reaching an instability (Macayeal, 1993), massive catastrophic outburst floods
58 from a glacially-dammed Hudson Strait (Johnson and Lauritzen, 1995), subglacial lake drainage
59 (Alley et al., 2006), ice shelf instability (Hulbe et al., 2004) or ice shelf collapse in response to
60 warming (Marcott et al., 2011), large tidal forces (Arbic et al., 2008), and ocean forcing (Bassis
61 et al., 2017). Each hypothesis involves MIS 3 North American Ice Sheet dynamics, since ice-
62 rafted debris carried by icebergs is derived from land formerly beneath the Laurentide Ice Sheet
63 (Hemming, 2004); however, the ice sheet's exact relationship to Heinrich events is debated
64 (Rashid and Piper, 2007; Rashid et al., 2019).



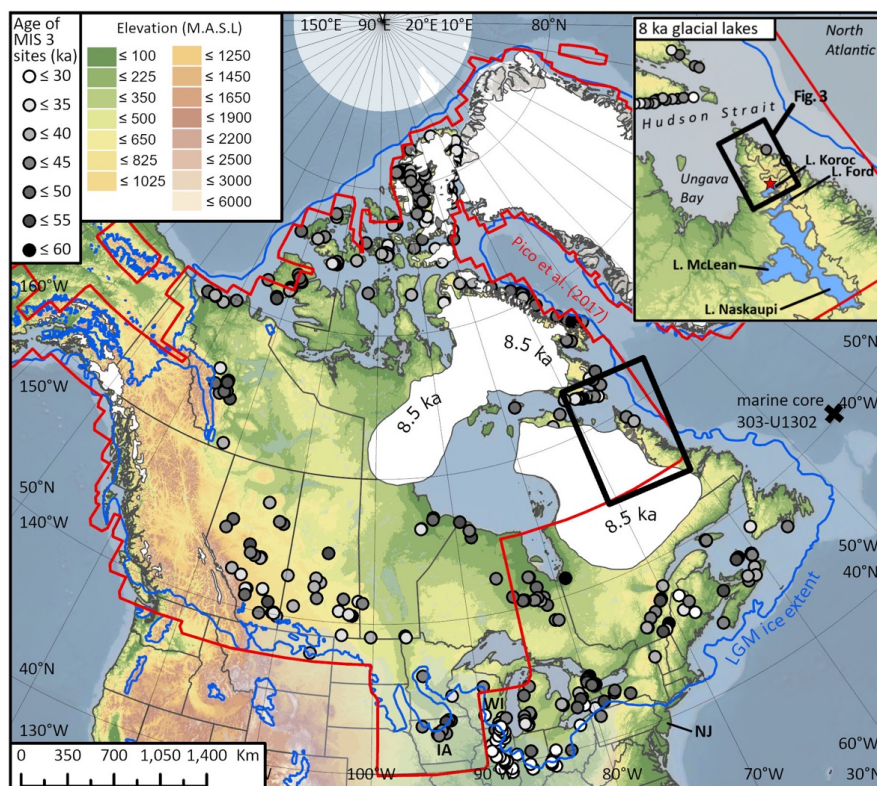
65

66

67 Figure 1 | A. $\delta^{18}O$ record from core 303-U1302 B. ice rafted debris (IRD) proxy, Gamma Ray Attenuation density
 68 (Channell et al., 2012) C. Atlantic Meridional Overturning Circulation (AMOC) proxy, Pa/Th ratio (Henry et al.,
 69 2016; McManus et al., 2004) D. Equivalent global mean sea level associated with the ICE-PC2 ice history (Pico et
 70 al., 2017) used to calculate glacial isostatic adjustment correction globally (black) and for the Laurentide Ice Sheet
 71 (blue). Purple bar shows shoreline age uncertainty (33-59 ka; minimum age = 36 ± 3 ka, likely age corrected for



72 burial = 56 ± 3 ka). Shaded purple bar encompasses Marine Isotope 3 (MIS 3; 60-26 ka) and vertical dashed black
 73 line note the timing of Heinrich events.



74
 75 Figure 2 | Map showing the study area (black rectangle) along with the approximate location of the Laurentide Ice
 76 Sheet at ~8.5 ka yr cal. BP, which may serve as an analogue for creating ice-dammed lakes such as the one
 77 documented in this study (white; Dalton et al., 2020). The locations of MIS 3 materials spanning 60 ka to 25 ka are
 78 also shown (points; Dalton et al., 2019), along with the 44-ka ice margin from Pico et al. (2017). Marine core 303-
 79 U1302 location is shown by a black cross (Channell et al., 2012). Elevation data from United States Geological
 80 Survey's Center for Earth Resources Observation and Science (EROS 2010) and continental shelf data from
 81 <http://www.naturalearthdata.com/>. NJ= New Jersey, WI= Wisconsin, IA=Iowa. Inset shows the location of
 82 deglacial 8 ka glacial lakes in the Torngat Mountains region, including glacial lake Koroc, glacial lake McLean, and



83 glacial lake Naskaupi from Dube-Loubert et al. (2018). The black rectangle shows study area included in Figure 3
84 and red star is the study site.

85

86 MIS 3 Laurentide Ice Sheet

87 The precise configuration of the Laurentide Ice Sheet during the interval leading into the Last
88 Glacial Maximum (LGM) would help to elucidate the origin of Heinrich events and their
89 variability across MIS 3, especially the potential source areas for ice-rafted debris and/or
90 meltwater pulses (Hemming, 2004). Although documenting the growth of the Laurentide Ice
91 Sheet is challenged by the sparsity of preserved records, recent work has refined Laurentide Ice
92 Sheet extent and volume during MIS 3. In particular, there is an increasing number of non-
93 glacial deposits in the Hudson Bay lowlands (Dalton et al., 2016), St. Lawrence lowlands (Parent
94 et al., 2015), Repulse Bay (Mcmartin et al., 2019), New England (Munroe et al., 2016), and
95 Atlantic Canada (Remillard et al., 2017), dated between 60 and 35 ka (Figure 2). This evidence
96 suggests a substantially reduced ice sheet at ~50-35 ka relative to the LGM, with ice possibly
97 restricted to two separate domes over eastern and western Canada at that time (Dalton et al.,
98 2019). However, concerns have been raised about the robustness of these chronologies, in
99 addition to the longstanding assumption that a large ice sheet is necessary to produce Heinrich
100 events (Miller and Andrews, 2019).

101

102 Regardless of the configuration of the Laurentide Ice Sheet between ~50-35 ka, there is
103 evidence for glacial advance towards maximum extent by ~45-35 ka in various locations. Key
104 pieces of evidence come from the dating of moraine deposits in Wisconsin (40-35 ka; Carlson et
105 al., 2018; Ceperley et al., 2019), sub-till organic-bearing deposits in Iowa (45 and 35 ka; Kerr et



106 *al.*, 2021), and evidence for abrupt blockage of northward water drainage in the eastern United
107 States around this time (~38 ka; Karig and Miller, 2013). In combination, these datasets suggest
108 either a rapidly advancing ice sheet from a Hudson Bay ice dome or a substantially revised ice
109 sheet arrangement that entails many separate ice caps.

110

111 Building on this observational evidence, glacial isostatic adjustment (GIA) analysis using
112 anomalously high sea-level markers along the United States mid-Atlantic dated to 50-35 ka
113 supports a late and rapid eastern Laurentide glaciation, suggesting that Laurentide ice volumes
114 increased four-fold from mid-MIS 3 to the LGM (Figure 1D; Pico et al., 2017). GIA analyses
115 based on sea-level records located on the ice sheet's peripheral bulge can determine total ice
116 volume in a given region, but not the precise geographic distribution. For example, although
117 there is evidence for a reduced MIS 3 Laurentide Ice Sheet, it cannot be determined whether
118 the Torngat Mountains, in northern Quebec and Labrador, were glaciated during MIS 3 (Pico et
119 al., 2018). Dynamic ice-sheet modeling studies implicate the Torngat Mountains as a site of
120 glacial inception (Otieno and Bromwich, 2009).

121

122 Following the notion that the Torngat Mountains were a key area of glacial inception through
123 the Quaternary (Koerner, 1980; Ives, 1957), this region is often depicted as fully glaciated
124 throughout MIS 3 (Batchelor et al., 2019), as well as across the entire interval of the last
125 glaciation phase, even during interstadials such as MIS 5a and 5c (Stokes et al., 2012).
126 Understanding the extent of glaciation in the Torngat Mountains is thus key to developing a
127 unified time-space history of Laurentide Ice Sheet growth because of its critical location as the



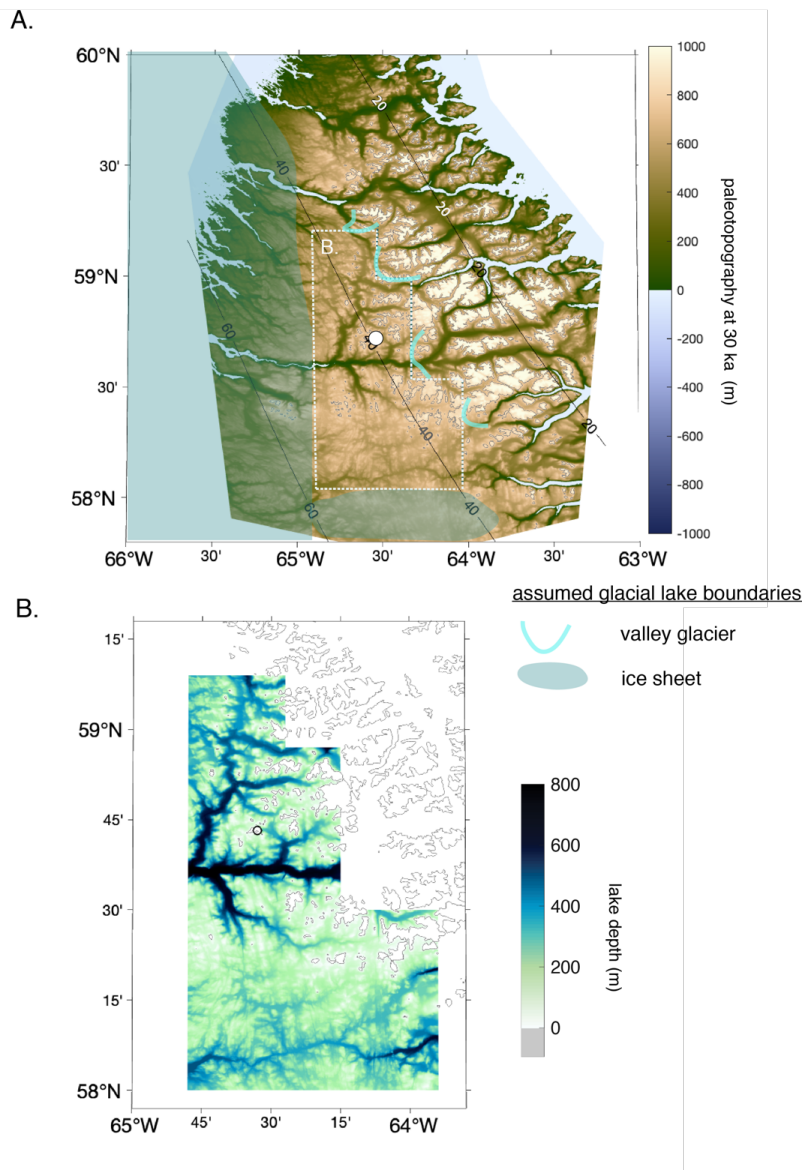
128 assumed site of inception for the Labrador Dome. However, only two shell ages on the Labrador
129 coastline, dated with conventional radiocarbon methods, exist as MIS 3 ice sheet constraints
130 (Figure 2). At present, no dated geologic constraints on MIS 3 ice sheet cover exist in the high-
131 elevation regions of the Torngat Mountains.

132

133 Here we report previously unpublished data from legacy fieldwork suggesting an MIS 3 glacial
134 lake and outburst flood in the Torngat Mountains (pre-LGM glacial lake Koroc, Figure 3). This
135 evidence, including ^{10}Be ages on a wave-cut shoreline, puts forth a series of testable
136 hypotheses about MIS 3 Laurentide configuration and Heinrich events. Did extensive valley
137 glaciers bound this glacial lake during MIS 3? Were high elevation regions of the Torngat
138 Mountains glaciated across MIS 3? Did glacial outburst floods coincide with Heinrich events?
139 How large could glacial outburst floods have been in the Torngat Mountains?

140

141 This evidence for glacial lake outburst flooding in the Torngat mountains calls for deeper
142 investigation via additional fieldwork, which could constrain the ice margins and quantify the
143 freshwater flux associated with MIS 3 Torngat outburst floods. The presence of an MIS 3 glacial
144 lake would preclude a full glaciation of the Torngat Mountains and would suggest freshwater
145 from an outburst flood drained into the Hudson Strait, through Ungava Bay. We explore
146 possible implications for MIS 3 Heinrich events by calculating the freshwater flux associated
147 with such a glacial outburst flood using high-resolution digital elevation maps corrected for
148 glacial isostatic adjustment.



149

150 Figure 3 | A. Paleotopography of study region corrected for glacial isostatic adjustment at 36 ka. Labeled contours
151 note relative sea-level change due to glacial isostatic adjustment (positive values are higher relative sea level, or
152 equivalently lower topography). The assumed glacial lake boundary is shown by a dashed white line, and the shaded
153 region shows the assumed ice sheet location. Blue curves show the assumed location of blockage by valley glaciers.



154 B. Calculated lake depth in pre-LGM glacial lake Koroc. White circle shows location age is measured on lake
 155 shoreline.

156

157

158 **METHODS**

159 Field setting

160 The Torngat Mountains in north-central Quebec and Labrador form a narrow, north–south-
 161 trending, high spine that weaves above a gently westward-dipping (0.8°) subsummit plateau
 162 (Figure 3A). East–west trending valleys cut across the plateau, which is currently covered by
 163 frost-riven felsenmeer fields and dotted by towering tors. The macroscale features represent a
 164 palimpsest landscape with formative valley incision dating to the Mesozoic era (Centeno, 2005),
 165 now bearing evidence of modification by Quaternary glaciation.

166

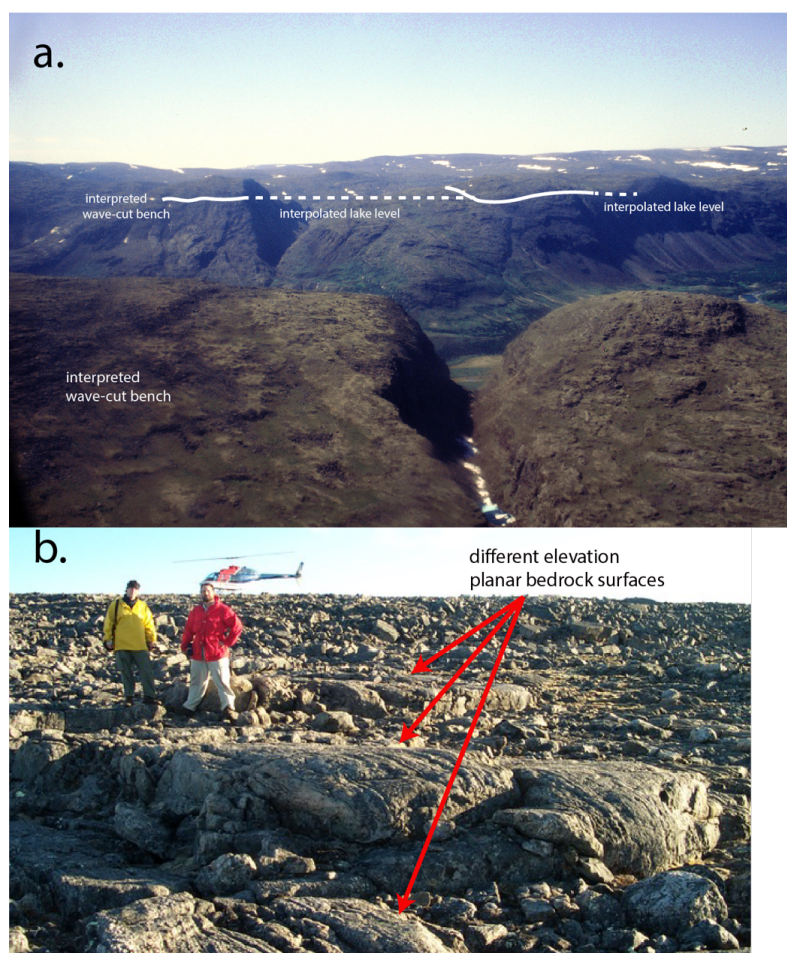
167 The Torngat’s U-shaped valleys are rife with flutes, moraines, roches moutonnées, striations and
 168 other indicators of the glacial and deglacial history. These attracted exploration and research
 169 from various landscape historians (Ives, 1958; Ives et al., 1978; Clark, 1987; Clark et al., 2000;
 170 Jansson, 2003; Jansson and Kleman, 2004; Barnett and Peterson, 1964; Staiger et al., 2005;
 171 Dube-Loubert et al., 2018; Andrews, 1973; Gray et al., 1993; Marquette et al., 2004). Ives
 172 (1958; 1978) interpreted the “weathering zones” above the valleys as trimlines of older, more
 173 voluminous glaciations. Later, Marquette et al.(2004) and Staiger et al.(2005) documented the
 174 presence of LGM-aged erratic boulders perched on older, angular felsenmeer slabs at high
 175 elevations, indicating that all but perhaps the highest few peaks $>1800\text{m}$ were ice-covered. This
 176 observation was corroborated using cosmogenic burial dating of the plateau surfaces that indicate



177 a complex burial history consistent with several phases of waxing and waning ice domes – the
178 last of which included a dome of the LIS likely centered on Ungava Bay (Staiger et al., 2005).
179
180 In the most recent deglaciation, the retreating margin dammed meltwater from flowing to the
181 ocean, forming large glacial lakes with shorelines around 500 m asl at its fullest extent in more
182 extensive lakes to the south in the George River valley, including Lake Naskaupi and Lake
183 McLean (Jansson, 2003; Allard et al., 1989; Jansson and Kleman, 2004; Rice et al., 2019).
184 Shorelines associated with Glacial Lake Naskaupi have been well-mapped and were dated to 8.3
185 ka using cosmogenic nuclide exposure dating (Dube-Loubert et al., 2018; Dube-Loubert and
186 Roy, 2017). Subsequently, these low-elevation lakes drained when the ice thinned enough to
187 allow them to release meltwater into Ungava Bay. Draining of Glacial Lake Koroc, Glacial Lake
188 Naskaupi, and other nearby glacial lakes into Ungava Bay (in addition to drainage of Glacial
189 Lake Agassiz and Ojibway into the Hudson Bay (Barber et al., 1999), has been invoked as
190 potential meltwater sources to trigger the 8.2 ka cold episode recorded in Greenland ice cores
191 (Jansson and Kleman, 2004).
192
193 The “intermediate zone” - between the high elevation peaks/plateau and the glacial valleys -
194 contain incipient felsenmeer, lacustrine beach sediments, and glacial drift covering bedrock with
195 scant evidence of glacial erosion. To our knowledge, indicators of high elevation lakes in the
196 Torngat Mountains have not been previously documented in the literature. This study considers
197 the outlines of an individual glacial lake in the “intermediate zone” at 890 m elevation in
198 Labrador-Ungava, Canada in the present-day Kuururjuaq National Park in Québec, Canada. This



199 glacial lake was identified based on geomorphological mapping of shorelines, spillways, and
200 drainage channels containing rounded cobbles and gravel entering the lake at high elevation.
201
202 Cosmogenic dating
203 During a 2002 field campaign, two locations were sampled to determine ^{10}Be ages on bedrock
204 surfaces from a well-developed shoreline at 890 m elevation (Figure 3; white circle). The
205 shoreline is an erosional feature, and there is a small inlet channel at this elevation with rounded,
206 imbricated cobbles, suggestive of outburst flooding (Figure 4).
207



208

209 Figure 4 | A. Photograph of view above interpreted wave-cut bench shoreline with high elevation shoreline visible
 210 across the valley. B. Photograph of planar bedrock surfaces with people for scale. Photographs courtesy of J.
 211 Willenbring and J. Gray.

212

213 Samples were collected from the gneissic bedrock wave-cut bench, whose surface did not appear
 214 highly weathered, using a hammer and chisel. The highest level of the lake was ~3m above the
 215 sample location. The lowest wave-cut bench level at this elevation was chosen in order to sample
 216 deeper into the cosmogenic nuclide production zone, thus minimizing inherited ^{10}Be in the
 217 bedrock in this area (Staiger et al., 2005). Samples were collected in 2002, as part of the field



218 campaign reported in Staiger et al. (2005). Sample preparation and quartz separation were
219 carried out according to standard laboratory protocols developed at the Dalhousie Cosmogenic
220 Dating Laboratory (Willenbring Staiger, 2005). The $^{10}\text{Be}/^9\text{Be}$ ratios were measured at Center for
221 Accelerator Mass Spectrometry at the Lawrence Livermore National Laboratory (California,
222 USA). Ages were calculated with version 3 of the online calculator
223 (<http://hess.ess.washington.edu/>) Uncertainties reflect 2σ analytical uncertainties (external
224 uncertainties) in the AMS analyses. Be carrier is from a shielded beryl, prepared by J. Klein.
225 Chemical blanks from the lab at that time ranged from 1.9×10 to 3.9×10 Be atoms. AMS was
226 completed at the at Lawrence Livermore National Laboratory (LLNL). AMS targets were
227 prepared at Dalhousie University. Concentrations were normalized to SLHL production rate in
228 order to compare samples from differing locations.

229

230 The reported ages assume no erosion or ice cover. Many processes control cosmogenic nuclide
231 production including erosion, burial by snow or vegetation, and changing atmospheric
232 concentrations(Gosse and Phillips, 2001). Although the history of ice burial and erosion is
233 unknown, based on prior regional studies, the apparent exposure age at our site's elevation of
234 890 m is likely less than 20 ky (Staiger et al., 2005). We considered the impact of GIA-induced
235 subsidence on our age calculation(Jones et al., 2019). Nevertheless, this correction is small
236 (~100s years) compared to age uncertainty related to ice cover or erosion, and thus we did not
237 quantify an age correction for GIA.

238

239

240 Glacial isostatic adjustment simulations



241 To reconstruct paleotopography during MIS 3 we simulate sea-level (or equivalently
242 topographic) change using gravitationally self-consistent glacial isostatic adjustment modeling.
243 Our calculations are based on the theory and pseudo-spectral algorithm described by Kendall et
244 al. (2005) with a spherical harmonic truncation at degree and order 256. These calculations
245 include the impact of load-induced Earth rotation changes on sea level (Milne & Mitrovica,
246 1996), evolving shorelines and the migration of grounded, marine-based ice (Johnston, 1993;
247 Milne et al., 1999; Lambeck et al., 2003; Kendall et al., 2005). Our predictions require models
248 for Earth's viscoelastic structure and the history of global ice cover. We adopt the viscosity
249 profile VM2, and ice history ICE-PC2, which is characterized by a rapid growth of the eastern
250 Laurentide Ice Sheet from 44 to 26 ka (Pico et al., 2017). We calculate paleotopography at 36 ka
251 and 56 ka by subtracting the simulated sea-level change from the present-day regional digital
252 elevation model.

253

254 Glacial lake volume calculation

255 We extracted a 0.75 arc second resolution digital elevation model from the Canadian Digital
256 Elevation Model project (<https://maps.canada.ca/czs/index-en.html>) of the region shown in
257 Figure 3. The glacial lake shoreline feature was measured at 890 m elevation. Lake extent was
258 delineated by assuming an ice margin to the southwest similar to where the 8 ka Glacial lake
259 Koroc shorelines are inferred (Figure 2 inset; Figure 3A; shaded blue). Because this lake is at
260 high elevation, it is not presently bounded to the east by higher topography. We assumed that
261 valley glaciers (long-recognized to have existed regionally during glaciations; Ives, 1958),
262 descended from these high elevation regions, and this glacial ice would have bounded this



263 glacial lake during MIS 3 (Figure 3A; blue lines). Pre-LGM glacial Lake Koroc is defined by
264 rectangular bounds in our study for simplicity (Figure 3; dashed white line), given that MIS 3 ice-
265 dam locations are unknown. We reconstructed paleotopography at 36 ka by correcting for sea-
266 level (or equivalently topographic) change using gravitationally self-consistent glacial isostatic
267 adjustment modeling (contours; Figure 3A). We calculated the lake volume by summing the
268 area multiplied by the water depth in each grid cell.

269

270 **RESULTS & DISCUSSION**

271

272 Glacial lake shoreline age

273 An age of 36 ± 3 ka is calculated assuming a continuous exposure with no erosion or burial
274 (Supplementary Table 1), and therefore may be considered a minimum exposure duration.
275 Erosion of exposed surfaces removes built-up cosmogenic nuclides, and ice cover reduces
276 cosmic ray exposure. Fully accounting for these processes is not possible, but would lead to
277 older exposure ages (Jones et al., 2019). Similar elevation sites nearby in the Torngat Mountains
278 studies have a maximum apparent exposure age (combined history of erosion and ice cover) of
279 20 ky (Staiger et al., 2005).

280

281 Although the duration of ice cover at this site is unknown, there is evidence for ice cover at the
282 LGM (Staiger et al., 2005), and this region likely deglaciated between 11 and 8 ka (Dalton et al.,
283 2020). The age correction for ice burial depends on the timing of glaciation, which occurred after
284 the existence of pre-LGM glacial lake Koroc. For example, if ice advanced over our site at 30 ka
285 and the entire area was glaciated until 10 ka, then there would have been 20 ky of ice cover,



286 which would shift the age to 56 ka. We therefore consider 36 ± 3 ka to represent a minimum age,
287 and 56 ± 3 ka a likely age for the identified pre-LGM glacial lake Koroc. Future work could
288 include measuring the ratio of two cosmogenic nuclides, such as paired $^{26}\text{Al}/^{10}\text{Be}$ isotope data.
289 Such paired isotope data would improve our understanding of ice burial and erosional history at
290 this site, better constraining the chronology of this wave-cut shoreline feature and granting
291 insight into the longer-term exposure history.

292

293 How would this glacial lake shoreline feature have been preserved? The presence of non-erosive
294 cold-based ice could have allowed the preservation of this wave-cut bench and small channel
295 with imbricated rounded cobbles. Felsenmeer has been documented at this elevation range in the
296 Torngat Mountains, which suggests the presence of a cold-based ice sheet (Staiger et al., 2005).
297 Future fieldwork could include mapping of shoreline features across this valley, and other
298 valleys within the Koroc River area. Other glacial lake outlets likely existed, and mapping these
299 features would better quantify the history of flood routing.

300

301 Glacial lake outburst volume estimate

302 We calculated the possible freshwater volume associated with an outburst flood event from the
303 pre-LGM glacial lake Koroc based on an 890 m elevation glacial lake shoreline (white circle;
304 Figure 3) and assumed ice-dammed locations (dashed white line; Figure 3). A shoreline elevation
305 of 851 m at 36 ka was determined by subtracting 39 m, the magnitude of topographic change at
306 36 ka due to glacial isostatic adjustment at this site (Figure 3A; contours).

307



308 Figure 3B shows the lake depth associated with the reconstructed extent of the pre-LGM glacial
309 lake. This calculation results in a glacial lake water volume of $1.14 \times 10^{12} \text{ m}^3$. If a glacial lake
310 outburst flood of this magnitude lasted three days (within the range of typical glacial outburst
311 flood (jokulhaup) duration; Bjornsson, 2010), a freshwater flux of 0.004 Sv ($1 \text{ Sv} = 10^6 \text{ m}^3/\text{s}$)
312 would drain to the Hudson Strait. Nevertheless, the duration of such an outburst flood could vary
313 substantially from present-day typical durations depending on the size of the drained lake. We
314 also calculated lake volume using GIA-corrected topography at 56 ka, to account for age
315 uncertainty, which results in an equivalent value of $1.14 \times 10^{12} \text{ m}^3$. Calculating the lake volume
316 without accounting for GIA resulted in a 7% smaller volume, with a value of $1.13 \times 10^{12} \text{ m}^3$.
317
318 We used an 890 m contour on present-day topography to determine lake extent and simplified
319 assumptions about ice-dammed locations. However, lake extent is uncertain as ice sheet margins
320 for this time interval are unknown. Nevertheless, ice thickness must have been over 1.1 times the
321 lake depth to be grounded and dam the glacial lake (Weertman, 1974; Schoof, 2007). Although
322 the presence of a glacial lake during MIS 3 suggests smaller ice sheet heights than previously
323 assumed in the Torngat Mountains, ice must have been sufficiently thick to create a glacially-
324 dammed lake. Could alpine glaciers be sufficiently thick to block such a lake? How thick would
325 the eastern ice margin need to be to block this lake? Future work, including mapping the full
326 extent of this glacial lake, could help answer these questions. In particular, it may be possible to
327 determine the minimum required ice thickness necessary to dam measured lake depths, as
328 determined by topography at shoreline locations.
329



330 Another uncertainty in our analysis is that we do not consider how topography may have
331 changed due to erosion. For example, there is evidence for at least 2.5 m of erosion in the valley
332 bottoms of the Torngat Mountain region over a single glacial cycle (Staiger et al., 2005), and
333 glacial outburst floods can cause substantial incision (Keisling et al., 2020; Larsen and Lamb,
334 2016). Future work aimed at reconstructing topography prior to landscape erosion may also
335 improve estimates of glacial lake volume.

336

337 Heinrich events

338 A freshwater volume of $1.14 \times 10^{12} \text{ m}^3$, associated with the glacial lake outburst described in this
339 study, could contribute to the large $\delta^{18}\text{O}$ recorded for MIS 3 Heinrich events (minimum volume
340 required = $1.4 \times 10^{13} - 2.3 \times 10^{14} \text{ m}^3$; Hemming, 2004). Outburst flooding from the ice-dammed
341 lake identified in this study would have drained westward through Ungava Bay into the Hudson
342 Strait and released a substantial volume of freshwater into the North Atlantic, likely carrying ice-
343 rafted debris.

344

345 Our estimated freshwater volume may represent a minimum bound. Glacial lakes in the Koroc
346 Valley existed during the Holocene, concurrent with larger lakes, including Lake Naskaupi and
347 Lake McLean, to the south, which have been dated to 8 ka (Dube-Loubert et al., 2018) (Figure 2;
348 inset). Thus, other pre-LGM glacial lakes likely existed to the south of the identified pre-LGM
349 glacial lake Koroc, similar to during the Holocene (Dube-Loubert et al., 2018), and could have
350 released their freshwater at a similar time during MIS 3. Each of these glacial lakes, including
351 glacial Lake Koroc, may have flooded repeatedly depending on the timescale of meltwater
352 refilling and ice dam lifting.



353

354 The age uncertainty of this glacial lake shoreline (33-59 ka), and its associated outburst flood,
355 spans the time period of multiple Heinrich events (Figure 1). As opposed to an ice discharge
356 event, floodwaters would introduce substantial freshwater but not carry ice rafted debris as far.
357 However, given age uncertainty, it is also possible this outburst flooding coincided with times
358 that are not associated with Heinrich events.

359

360 Previously proposed hypotheses for Heinrich events (ice-sheet instability/tides/jokulhaups)
361 invoke specific assumptions about Laurentide ice sheet dynamics or configurations. However,
362 to-date, evidence on land beneath the former ice sheet could not sufficiently support or refute
363 these ideas. We present the first direct evidence on land for an MIS 3 jokulhaup. The shoreline
364 age uncertainty in our study encompasses multiple Heinrich events, and suggests the possibility
365 of outburst flooding as a mechanism for one of these climatic events. This early dataset
366 motivates future fieldwork that could test the hypothesis that a jokulhaup in the Torngat
367 Mountains coincided with a Heinrich event. Further investigation mapping glacial lake extent
368 would better quantify the volume associated with such a glacial outburst flood.

369

370 Ice sheet constraints

371 The pre-LGM glacial lake Koroc shoreline, with a minimum age of 36 ± 3 ka, is the first evidence
372 to suggest that the Torngat Mountains were not fully glaciated across MIS 3, and has the
373 potential to grant insight into MIS 3 Laurentide ice margins as well as the mechanisms
374 underlying glacial inception in North America. Although we cannot infer the precise locations
375 where ice dammed this lake, we know that, during the Holocene, glacial lakes existed in the



376 lower elevation Koroc River valley in addition to farther south, such as Lake Naskaupi (Dube-
377 Loubert et al., 2018) (Figure 2; inset). These 8 ka glacial lakes, surrounding the retreating
378 remainder of the Laurentide Ice Sheet, occurred at a time when the Laurentide Ice Sheet held 4 m
379 of equivalent global mean sea level (Ullman et al., 2016), a fraction of the ~80 m global mean
380 sea level equivalent the Laurentide Ice Sheet held at the LGM (Figure 1d). Despite similar
381 glacial lake locations, however, mid-MIS 3 ice margins were not necessarily the same as at 8 ka,
382 and caution is required in interpreting ice volumes associated with an ice margin proximal to pre-
383 LGM glacial lake Koroc. Higher water levels in the pre-LGM glacial lake Koroc (890 m
384 compared to ~500 m at 8 ka) suggest greater ice thickness at the margin. Therefore, although the
385 mid-MIS 3 ice sheet margin may have been close to the 8-ka margin near the Torngat
386 Mountains, the ice cap may have been more extensive to the west at the time of this MIS 3
387 glacial lake than it was at 8 ka.

388

389 Nonetheless, our study suggests that the Torngat Mountains were not fully glaciated across MIS
390 3. This finding is in contrast to numerical ice sheet modeling studies and other ice sheet
391 reconstructions, which predict that this region is one of the first to glacial (Otieno and
392 Bromwich, 2009) and would have remained glaciated through the Last Glacial Maximum
393 (Stokes et al., 2012). Assumptions about glacial climate used in dynamic ice-sheet simulations
394 based on global circulation models may require revision to fit constraints for a reduced mid-MIS
395 3 Laurentide Ice Sheet, and an unglaciated sector (of at least part) of the Torngat Mountains at
396 MIS 3.

397



398 The location of pre-LGM glacial lake Koroc in the Torngat Mountains supports a rapidly-
399 growing ice sheet, given that maximum ice sheet extent was reached on the United States east
400 coast by 27-25 ka (Corbett et al., 2017) and the United States Midwest by 45-35 ka (Carlson et
401 al., 2018; Kerr, 2018; Ceperley *et al.*, 2019). This finding would support a dynamic Laurentide
402 Ice Sheet in the period leading to the Last Glacial Maximum. Rather than a single growing mass,
403 this ice sheet may have encompassed a series of temporally variable ice caps in various centers
404 such as the Appalachians, Mid-Quebec, as well as the larger domes in Keewatin and Labrador.

405

406 CONCLUSION

407 In this study we provide the first direct on-land evidence for an MIS 3 glacial outburst flood. We
408 present cosmogenic exposure ages from legacy fieldwork for a glacial lake shoreline with
409 evidence for outburst flooding, with a minimum age of 36 ± 3 ka in the Torngat Mountains. This
410 previously unpublished dataset weighs into debates about the Laurentide Ice Sheet and Heinrich
411 events during MIS 3.

412

413 We suggest a series of hypotheses based on these observations: Were high elevation regions of
414 the Torngat Mountains, at least partially, deglaciated during MIS 3? Could glacial outburst
415 floods in the Torngat Mountains have coincided with Heinrich events in the North Atlantic? How
416 large and how frequent were Torngat Mountain glacial outburst floods? Future work, including
417 thorough mapping of MIS 3 glacial lake shorelines in the Torngat Mountains and an improved
418 burial history from paired cosmogenic isotopes can begin to answer these questions.
419 Furthermore, tracking pre-LGM glacial lake shorelines and documenting glacial lake tilts, in



420 combination with glacial isostatic adjustment modeling, can begin to tease out ice sheet
421 dynamics during the glaciation phase of North America.

422

423 **ACKNOWLEDGMENTS**

424 T.P acknowledges funding from UC President's Postdoc Fellowship and NSF EAR Postdoctoral
425 Fellowship. J.K.W. acknowledges the GSC TFSS for field equipment during mapping and
426 sample collection. Field access was partly supported by the Canadian Coast Guard. This research
427 was supported by a Killam Fellowship and an NSF-OPP (Grant OPP-9906280) and ACOA-AIF
428 (Grant 1005052) to J. Gosse.

429

430 **Author contribution & Competing Interests:**

431

432 T.P performed glacial isostatic adjustment modeling and lake volume calculation. T.P prepared
433 the manuscript with contributions from all coauthors. J.K.W. carried out fieldwork, sample
434 collection, and cosmogenic nuclide laboratory work and analysis. All coauthors contributed
435 conceptually to the development of this manuscript. The authors declare that they have no
436 conflict of interest.

437

438 **REFERENCES**

439

440 Allard, M., Fournier, A., Gahé, E., and Seguin, M. K.: Le Quaternaire de la cote sud-est de la baie
441 d'Ungava, Quebec nordique, Geogr. Phys. Quat., 1989.
442 Alley, R., Dupont, T. K., Lawson, D. E., and Evenson, E. B.: Outburst flooding and the initiation of
443 ice-stream surges in response to climatic cooling : A hypothesis,



- 444 <https://doi.org/10.1016/j.geomorph.2004.01.011>, 2006.
- 445 Andrews, J. T.: The Wisconsin Laurentide Ice Sheet : Dispersal Centers , Problems of Rates of
- 446 Retreat , and Climatic Implications, *Arct. Alp. Res.*, 5, 185–199, 1973.
- 447 Arbic, B. K., Mitrovica, J. X., Macayeal, D. R., and Milne, G. A.: On the factors behind large
- 448 Labrador Sea tides during the last glacial cycle and the potential implications for Heinrich
- 449 events, *Palaeogeogr. Palaeoclim. Palaeoecol.*, 23, 1–14,
- 450 <https://doi.org/10.1029/2007PA001573>, 2008.
- 451 Barber, D. C., Jennings, A. E., Andrews, J. T., Kerwin, M. W., and Morehead, M. D.: Forcing of the
- 452 cold event of 8 , 200 years ago by catastrophic drainage of Laurentide lakes, 400, 13–15, 1999.
- 453 Barnett, D. M. and Peterson, J. A.: The significance of Glacial Lake Naskaupi 2 in the deglaciation
- 454 of Labrador-Ungava, *Can. Geogr.*, 000, 173–181, 1964.
- 455 Bassis, J. N., Petersen, S. V., and Cathles, L. Mac: Heinrich events triggered by ocean forcing and
- 456 modulated by isostatic adjustment, *Nature*, 5–7, <https://doi.org/10.1038/nature21069>, 2017.
- 457 Batchelor, C. L., Margold, M., Krapp, M., Murton, D. K., Dalton, A. S., Gibbard, P. L., Stokes, C. R.,
- 458 Murton, J. B., and Manica, A.: The configuration of Northern Hemisphere ice sheets through the
- 459 Quaternary, *Nat. Commun.*, 10, 1–10, <https://doi.org/10.1038/s41467-019-11601-2>, 2019.
- 460 Björnsson, H.: Understanding jokulhlaups : from tale to theory, *J. Glaciol.*, 56, 1002–1010, 2010.
- 461 Bond, G., Broecker, W., Johnsen, S., Mcmanus, J., Labeyrie, L., Jouzel, J., and Bonani, G.:
- 462 Correlations between climate records from North Atlantic sediments and Greenland ice,
- 463 *Nature*, 143–147, 1993.
- 464 Carlson, A. E., Tarasov, L., and Pico, T.: Rapid Laurentide ice-sheet advance towards southern
- 465 last glacial maximum limit during marine isotope stage 3, *Quat. Sci. Rev.*, 196, 118–123,



- 466 <https://doi.org/10.1016/j.quascirev.2018.07.039>, 2018.
- 467 Centeno, J. P.: Exhumation and Incision History of the Torngat Mountains, Northern Labrador
 468 and Quebeca, Canada, using apatite (U-Th)/He thermochronology, University of Kansas, 2005.
- 469 Ceperley, E. G., Marcott, S. A., Ili, J. E. R., Zoet, L. K., and Zimmerman, S. R. H.: The role of
 470 permafrost on the morphology of an MIS 3 moraine from the southern Laurentide Ice Sheet,
 471 *Geology*, 47, 440–444, 2019.
- 472 Channell, J. E. T., Hodell, D. A., Romero, O., Hillaire-marcel, C., de Vernal, A., Stoner, J. .,
 473 Mazaud, A., and Rohl, U.: A 750-kyr detrital-layer stratigraphy for the North Atlantic (IODP Sites
 474 A 750-kyr detrital-layer stratigraphy for the North Atlantic (IODP Sites U1302 – U1303 , Orphan
 475 Knoll , Labrador Sea), *Earth Planet. Sci. Lett.*, 317–318, 218–230,
 476 <https://doi.org/10.1016/j.epsl.2011.11.029>, 2012.
- 477 Clark, C. D., Knight, J. K., and Gray, J. T.: Geomorphological reconstruction of the Labrador
 478 Sector of the Laurentide Ice Sheet, *Quat. Sci. Rev.*, 19, 2000.
- 479 Clark, P. U.: Glacial geology of the Torngat Mountains , Labrador, *Can. J. Earth Sci.*, 11, 1987.
- 480 Corbett, L. B., Bierman, P. R., Stone, B. D., Caffee, M. W., and Larsen, P. L.: Cosmogenic nuclide
 481 age estimate for Laurentide Ice Sheet recession from the terminal moraine , New Jersey , USA ,
 482 and constraints on latest Pleistocene ice sheet history, *Quat. Res.*, 87, 482–498,
 483 <https://doi.org/10.1017/qua.2017.11>, 2017.
- 484 Dalton, A. S., Finkelstein, S. A., Barnett, P. J., and Forman, S. L.: Constraining the Late
 485 Pleistocene history of the Laurentide Ice Sheet by dating the Missinaibi Formation, Hudson Bay
 486 Lowlands, Canada, *Quat. Sci. Rev.*, 146, 288–299,
 487 <https://doi.org/10.1016/j.quascirev.2016.06.015>, 2016.



488 Dalton, A. S., Finkelstein, S. A., Forman, S. L., Barnett, P. J., Pico, T., and Mitrovica, J. X.: Was the
 489 Laurentide Ice Sheet significantly reduced during Marine Isotope Stage 3 ?, *Geology*, 47, 111–
 490 114, 2019.

491 Dalton, A. S., Margold, M., Stokes, C. R., Tarasov, L., Dyke, A. S., Adams, R. S., Allard, S., Arends,
 492 H. E., Atkinson, N., Attig, J. W., Barnett, P. J., Barnett, R. L., Batterson, M., Bernatchez, P., Borns,
 493 H. W., Breckenridge, A., Briner, J. P., Brouard, E., Campbell, J. E., Carlson, A. E., Clague, J. J.,
 494 Curry, B. B., Easterbrook, D. J., Franzi, D. A., Friedrich, H. G., Funder, S., Gauthier, M. S., Hooyer,
 495 T. S., Gowan, A. S., Harris, K. L., Bernard, H., Jennings, C. E., Johnson, M. D., Kehew, A. E., Kelley,
 496 S. E., Kerr, D., King, E. L., Kjeldsen, K. K., Knaeble, A. R., Lajeunesse, P., Lakeman, T. R., Lamothe,
 497 M., Larson, P., Lavoie, M., Loope, H. M., Lowell, T. V., Lusardi, B. A., Manz, L., Mcmartin, I.,
 498 Nixon, F. C., Occhietti, S., Parkhill, M. A., Piper, D. J. W., Pronk, A. G., Richard, P. J. H., Ridge, J.
 499 C., Ross, M., Roy, M., Seaman, A., Shaw, J., Stea, R. R., Teller, J. T., Thompson, W. B.,
 500 Thorleifson, L. H., Utting, D. J., Veillette, J. J., Ward, B. C., Weddle, T. K., and Wright, H. E.: An
 501 updated radiocarbon-based ice margin chronology for the last deglaciation of the North
 502 American Ice Sheet Complex, *Quat. Sci. Rev.*, 234,
 503 <https://doi.org/10.1016/j.quascirev.2020.106223>, 2020.

504 Dube-Loubert, H. and Roy, M.: Development , evolution and drainage of glacial Lake Naskaupi
 505 during the deglaciation of north-central Quebec and Labrador, *J. Quat. Sci.*, 32, 1121–1137,
 506 <https://doi.org/10.1002/jqs.2997>, 2017.

507 Dube-Loubert, H., Roy, M., Schaefer, J. M., and Clark, P. U.: Be dating of former glacial Lake
 508 Naskaupi (Quebec-Labrador) and timing of its discharges during the last deglaciation, *Quat. Sci.*
 509 *Rev.*, 191, 31–40, <https://doi.org/10.1016/j.quascirev.2018.05.008>, 2018.



- 510 Gosse, J. C. and Phillips, F. M.: Terrestrial in situ cosmogenic nuclides : theory and application,
 511 Quat. Sci. Rev., 20, 2001.
- 512 Gray, J. T., Lauriol, B., Bruneau, D., and Ricard, J.: Postglacial emergence of Ungava Peninsula ,
 513 and its relationship to glacial history, Can. J. Earth Sci., 30, 1993.
- 514 Hemming, S. R.: Heinrich Events: Massive Late Pleistocene detritus layers of the North Atlantic
 515 and their global climate imprint, Rev. Geophys., 42, <https://doi.org/10.1029/2003RG000128>,
 516 2004.
- 517 Henry, L. G., Mcmanus, J. F., Curry, W. B., Roberts, N. L., Piotrowski, A. M., Keigwin, L. D., and
 518 These, C.: North Atlantic ocean circulation and abrupt climate change during the last glaciation,
 519 Science (80-.), 353, 301–303, 2016.
- 520 Hulbe, C. L., Macayeal, D. R., Denton, G. H., Kleman, J., and Lowell, T. V: Catastrophic ice shelf
 521 breakup as the source of Heinrich event icebergs, Paleoceanography, 19, 1–16,
 522 <https://doi.org/10.1029/2003PA000890>, 2004.
- 523 Ives, J. D.: Glaciation of the Torngat Mountains, Northern Labrador, Arct. Inst. North Am., 10,
 524 1957.
- 525 Ives, J. D.: Glacial Drainage Channels as Indicators of Late-glacial Conditions in Labrador-
 526 Ungava: a Discussion, Cah. Geogr. Que., 3, 57–72, <https://doi.org/10.7202/020113ar>, 1958.
- 527 Ives, J. D., Arctic, S., Mar, N., and Ives, J. D.: The Maximum Extent of the Laurentide Ice Sheet
 528 along the East Coast of North America during the Last Glaciation, Arct. Inst. North Am., 31, 24–
 529 53, 1978.
- 530 Jansson, K. N.: Early Holocene glacial lakes and ice marginal retreat pattern in Labrador /
 531 Ungava , Canada, Palaeogeogr. Palaeoclimatol. Palaeoecol., 193, 473–501,



- 532 [https://doi.org/10.1016/S0031-0182\(03\)00262-1](https://doi.org/10.1016/S0031-0182(03)00262-1), 2003.
- 533 Jansson, K. N. and Kleman, J.: Early Holocene glacial lake meltwater injections into the Labrador
- 534 Sea and Ungava Bay, *Paleoceanography*, 19, 1–12, <https://doi.org/10.1029/2003PA000943>,
- 535 2004.
- 536 Johnson, R. G. and Lauritzen, E.: Hudson Bay-Hudson Strait jokulhlaups and Heinrich events : a
- 537 hypothesis, *Palaeogeogr. Palaeoclim. Palaeoecol.*, 117, 1995.
- 538 Jones, R. S., Whitehouse, P. L., Bentley, M. J., Small, D., and Dalton, A. S.: Impact of glacial
- 539 isostatic adjustment on cosmogenic surface-exposure dating, *Quat. Sci. Rev.*, 212, 206–212,
- 540 <https://doi.org/10.1016/j.quascirev.2019.03.012>, 2019.
- 541 Karig, D. E. and Miller, N. G.: Middle Wisconsin glacial advance into the Appalachian Plateau
- 542 ,Sixmile Creek, Tompkins Co., NY, *Quat. Res.*, 80, 522–533, 2013.
- 543 Keisling, B. A., Nielsen, L. T., Hvidberg, C. S., Nuterman, R., and Deconto, R. M.: Pliocene –
- 544 Pleistocene megafloods as a mechanism for Greenlandic megacanyon formation, *Geology*, 48,
- 545 737–741, 2020.
- 546 Kerr, P.: Middle to early-late Wisconsin glaciation in north central Iowa: timing, distribution,
- 547 and implications for reconstructions of the Laurentide Ice Sheet during MIS 3, University of
- 548 Iowa, 2018.
- 549 Kerr, P. J., Tassier-surine, S. A., Kilgore, S. M., Bettis, E. A., Dorale, J. A., and Cramer, B. D.:
- 550 Timing , provenance , and implications of two MIS 3 advances of the Laurentide Ice Sheet into
- 551 the Upper Mississippi River Basin , USA, *Quat. Sci. Rev.*, 261, 106926,
- 552 <https://doi.org/10.1016/j.quascirev.2021.106926>, 2021.
- 553 Koerner, R.: Instantaneous Glacierization, the Rate of Albedo Change, and Feedback Effects at



- 554 the Beginning of an Ice Age., *Quat. Res.*, 13, 153–159, <https://doi.org/doi:10.1016/0033->
 555 5894(80)90025-3, 1980.
- 556 Larsen, I. J. and Lamb, M. P.: Progressive incision of the Channeled Scablands by outburst
 557 floods, *Nature*, 538, 229–232, <https://doi.org/10.1038/nature19817>, 2016.
- 558 Macayeal, D. R.: Binge/purge oscillations of the Laurentide Ice Sheet as a cause of the North
 559 Atlantic’s Heinrich events, *Paleoceanography*, 8, 775–784, 1993.
- 560 Marcott, S. A., Clark, P. U., Padman, L., Klinkhammer, G. P., Springer, S. R., Liu, Z., Otto-bliesner,
 561 B. L., Carlson, A. E., Ungerer, A., Padman, J., and He, F.: Ice-shelf collapse from subsurface
 562 warming as a trigger for Heinrich events, *Proc. Natl. Acad. Sci.*, 108, 13415–13419,
 563 <https://doi.org/10.1073/pnas.1104772108>, 2011.
- 564 Marquette, G. C., Gray, J. T., Gosse, J. C., Courchesne, F., Stockli, L., Macpherson, G., and Finkel,
 565 R.: Felsenmeer persistence under non-erosive ice in the Torngat and Kaumajet mountains ,
 566 Quebec and Labrador , as determined by soil weathering and cosmogenic nuclide exposure
 567 dating, *Can. J. Earth Sci.*, 41, 19–38, <https://doi.org/10.1139/E03-072>, 2004.
- 568 McManus, J. F., Francois, R., Gherardi, J., and Keigwin, L. D.: Collapse and rapid resumption of
 569 Atlantic meridional circulation linked to deglacial climate changes, *Nature*, 428, 1–4, 2004.
- 570 Mcmartin, I., Campbell, J. E., and Dredge, L. A.: Middle Wisconsinan marine shells near Repulse
 571 Bay , Nunavut , Canada : implications for Marine Isotope Stage 3 ice-free conditions and
 572 Laurentide Ice Sheet dynamics in north-west Hudson Bay, *J. Quat. Sci.*, 34, 64–75,
 573 <https://doi.org/10.1002/jqs.3081>, 2019.
- 574 Miller, G. H. and Andrews, J. T.: Hudson Bay was not deglaciaded during MIS-3, *Quat. Sci. Rev.*,
 575 225, 105944, <https://doi.org/10.1016/j.quascirev.2019.105944>, 2019.



576 Munroe, J. S., Perzan, Z. M., and Amidon, W. H.: Cave sediments constrain the latest
 577 Pleistocene advance of the Laurentide Ice Sheet in the Champlain Valley , Vermont , USA, J.
 578 Quat. Sci., 31, 893–904, <https://doi.org/10.1002/jqs.2913>, 2016.

579 Otieno, F. and Bromwich, D.: Contribution of Atmospheric Circulation to Inception of the
 580 Laurentide Ice Sheet at 116 kyr BP *, J. Clim., 39–57, <https://doi.org/10.1175/2008JCLI2211.1>,
 581 2009.

582 Parent, M., Lefebvre, R., Rivard, C., Lavoie, M., and Guilbault, J.-P.: Mid-Wisconsinan Fluvial and
 583 Marine Sediments In the Central St. Lawrence Lowlands - Implications for Glacial and Deglacial
 584 Events in the Appalachian Uplands, in: GSA Northeastern Section - 50th Annual meeting, 2015.

585 Pico, T., Creveling, J. R., and Mitrovica, J. X.: Sea-level records from the U.S. mid-Atlantic
 586 constrain Laurentide Ice Sheet extent during Marine Isotope Stage 3, Nat. Commun., 8, 15612,
 587 <https://doi.org/10.1038/ncomms15612>, 2017.

588 Pico, T., Birch, L., Weisenberg, J., and Mitrovica, J. X.: Refining the Laurentide Ice Sheet at
 589 Marine Isotope Stage 3 : A data-based approach combining glacial isostatic simulations with a
 590 dynamic ice model, Quat. Sci. Rev., 195, 171–179,
 591 <https://doi.org/10.1016/j.quascirev.2018.07.023>, 2018.

592 Rashid, H. and Piper, D. J. W.: The extent of ice on the continental shelf off Hudson Strait during
 593 Heinrich events 1 – 3 1, Can. J. Earth Sci., 1549, 1537–1549, <https://doi.org/10.1139/E07-051>,
 594 2007.

595 Rashid, H., Jw, D., Drapeau, J., Marin, C., and Smith, M. E.: Sedimentology and history of
 596 sediment sources to the NW Labrador Sea during the past glacial cycle, Quat. Sci. Rev., 221,
 597 105880, <https://doi.org/10.1016/j.quascirev.2019.105880>, 2019.



- 598 Remillard, A., St-onge, G., Bernatchez, P., Bernard, H., Audrey, M. R., Buylaert, J., Murray, A. S.,
 599 and Lajeunesse, P.: Relative sea-level changes and glacio-isostatic adjustment on the Magdalen
 600 Islands archipelago (Atlantic Canada) from MIS 5 to the late Holocene, *Quat. Sci. Rev.*, 171,
 601 216–233, <https://doi.org/10.1016/j.quascirev.2017.07.015>, 2017.
- 602 Rice, J. M., Ross, M., Paulen, R. C., Kelley, S. E., Briner, J. P., Neudorf, C. M., and Lian, O. B.:
 603 Refining the ice flow chronology and subglacial dynamics across the migrating Labrador Divide
 604 of the Laurentide Ice Sheet with age constraints on deglaciation, *J. Quat. Sci.*, 34, 519–535,
 605 <https://doi.org/10.1002/jqs.3138>, 2019.
- 606 Schoof, C.: Ice sheet grounding line dynamics : Steady states , stability , and hysteresis, *J.*
 607 *Geophys. Res.*, 112, 1–19, <https://doi.org/10.1029/2006JF000664>, 2007.
- 608 Seidenkrantz, M. S., Kuijpers, A., Sørensen, S. A., Lindgreen, H., Olsen, J., and Pearce, C.:
 609 Evidence for influx of Atlantic water masses to the Labrador Sea during the Last Glacial
 610 Maximum, *Sci. Rep.*, 1–14, <https://doi.org/10.1038/s41598-021-86224-z>, 2021.
- 611 Staiger, J. K. W., Gosse, J. C., Johnson, J. V., Fastook, J., Gray, J. T., Stockli, D. F., Stockli, L., and
 612 Finkel, R.: Quaternary relief generation by polythermal glacier ice, *Earth Surf. Process.*
 613 *Landforms*, 1159, 1145–1159, <https://doi.org/10.1002/esp.1267>, 2005.
- 614 Stokes, C. R., Tarasov, L., and Dyke, A. S.: Dynamics of the North American Ice Sheet Complex
 615 during its inception and build-up to the Last Glacial Maximum, *Quat. Sci. Rev.*, 50, 86–104,
 616 <https://doi.org/10.1016/j.quascirev.2012.07.009>, 2012.
- 617 Ullman, D. J., Carlson, A. E., Hostetler, S. W., Clark, P. U., Cuzzone, J., Milne, G. A., Winsor, K.,
 618 and Caffee, M.: Final Laurentide ice-sheet deglaciation and Holocene climate-sea level change,
 619 *Quat. Sci. Rev.*, 152, 49–59, <https://doi.org/10.1016/j.quascirev.2016.09.014>, 2016.



- 620 Weertman, J.: Stability of the Junction of an Ice Sheet and an Ice Shelf, *J. Glaciol.*, 13, 3–11,
621 <https://doi.org/10.3189/S0022143000023327>, 1974.
- 622 Willenbring Staiger, J.: Glacial Erosion in Atlantic and Arctic Canada Determined by Terrestrial In
623 Situ Cosmogenic Nuclides and Ice Sheet Modeling, Dalhousie University, 2005.
- 624